A&A manuscript no.
(will be inserted by hand later)

Your thesaurus codes are:
11 (05.03.1)

ASTRONOMY AND ASTROPHYSICS
August 25, 1999

The 3D Elliptic Restricted Three-Body Problem: periodic orbits which bifurcate from limiting restricted problems

Complex instability

Mercè Ollé and Joan R. Pacha

Dept. de Matemàtica Aplicada I. Universitat Politècnica de Catalunya, Diagonal 647,
08028 Barcelona, Spain.
email: olle@ma1.upc.es, joanr@vilma.upc.es

Received 19 April 1999 / Accepted 21 July 1999

Abstract. At the present work we use certain isolated symmetric periodic orbits found in some limiting Restricted Three-Body Problems to obtain, by numerical continuation, families of symmetric periodic orbits of the more general Spatial Elliptic Restricted Three Body Problem. In particular, the Planar Isosceles Restricted Three Body Problem, the Sitnikov Problem and the MacMillan problem are considered. A stability study for the periodic orbits of the families obtained – specially focused to detect transitions to complex instability –, is also made.

Key words: periodic orbits – continuation method – bifurcations – complex instability

1. Introduction

Complex instability is a typical phenomenon of periodic orbits in Hamiltonian systems with three or more degrees of freedom. At present we have a good, although not complete, understanding of the dynamics associated with it. Actually some papers have been devoted to its study in different dynamical models: galactic potentials (see Magnenat 1982a, 1982b; Pfenniger 1985b, 1987, 1990; Contopoulos 1986a, 1986b; Contopoulos & Barbanis 1985, 1994; Martinet et al. 1987, 1988; Cleary 1989; Patsis & Zachilas 1990, 1994; Ollé & Pfenniger 1998), 4-D symplectic mappings (Pfenniger 1985a; Contopoulos & Giorgilli 1988; Ollé & Pfenniger, 1998; Zachilas 1993), planetary systems (Hadjidemetriou 1985), the Circular Restricted Three-Body Problem (Ollé & Pacha 1998), rotating oscillators (Pfenniger 1987) and Quantum Dynamics (Contopoulos et al. 1994). There are also analytical results about the dynamics around a transition stability-complex instability (Heggie 1985; Bridges et al. 1995; Papadaki et al. 1995; Ollé et al. 1999), which state that a Hopf-like bifurcation is associated with such transition, that can be direct (there is a powerful confinement around the complex unstable orbit, and there bifurcate stable 2D tori on the unstable side) or inverse (sudden chaos appear on the unstable region and there bifurcate unstable 2D tori on the stable zone).

In this paper we study the 3D Elliptic Restricted Three-Body Problem (ERTBP): we consider two primaries with masses μ and $1-\mu$ (in suitable units), moving in a plane on Keplerian ellipses with eccentricity e, $0 \leq e \leq 1$; a fixed reference frame, with its origin at the common center of mass of the primaries is used. The Spatial Elliptic Restricted Three Body Problem consists of describing the motion of a particle, with infinitesimal mass and which does not affect the binary system, in the gravitational field created by the two primaries. To our knowledge the spatial problem remains to be well explored since there are few papers devoted to it: Katsiaris (1973) computed some periodic orbits in the range $e \in [0, 0.4]$ and $\mu \in [0.01, 0.015]$, Macris et al. (1975), in the range $e \in [0, 0.0175]$ and $\mu = 0.4$, and Gómez et al. (1992) detected the zone of stable motion in a vicinity of the equilateral points of the Earth-Moon system. This problem is a typical example of a *non-conservative* and non-integrable dynamical system of three degrees of freedom. Throughout the paper we shall assume that $\mu = 1/2$ (i.e., the primaries have equal masses); and, in an inertial frame and suitable units (such that the universal gravitational constant G, the maximum distance from one primary to the origin are both equal to one, and the period of the orbit of the primaries equals 2π), the motion of the particle in the ERTBP is given by the *non-autonomous* Hamiltonian

$$H(\boldsymbol{\xi}, \boldsymbol{\eta}, e; E) = \frac{1}{2}(1 + e\cos E)\left\{\|\boldsymbol{\eta}\|^2 - V(\boldsymbol{\xi}, e; E)\right\}, \qquad (1)$$

with $\boldsymbol{\xi} = (x_1, x_2, x_3)^{\mathrm{T}}$, $\boldsymbol{\eta} = (x_4, x_5, x_6)^{\mathrm{T}}$; being $x_{i+3} = x_i'$, $i = 1, 2, 3$ where the primes denote derivation with respect to the eccentric anomaly of the orbit of the primaries, E, introduced as the new independent variable, which is related with the time t by the Kepler equation:

$$t = E + e\sin E.$$

Send offprint requests to: Mercè Ollé

The function V in the above Hamiltonian is defined by,

$$V(\boldsymbol{\xi}, e; E) = \frac{1}{\|\boldsymbol{\sigma}_1\|} + \frac{1}{\|\boldsymbol{\sigma}_2\|},$$

where $\|\boldsymbol{\sigma}_1\|$, $\|\boldsymbol{\sigma}_2\|$ are the $\|\cdot\|_2$ norms of the vectors,

$$\boldsymbol{\sigma}_1 = \boldsymbol{\xi} - \boldsymbol{R}, \quad \boldsymbol{\sigma}_2 = \boldsymbol{\xi} + \boldsymbol{R},$$

and the vectors $\boldsymbol{R}$, $-\boldsymbol{R}$ give the position of the two primaries, i.e.:

$$\boldsymbol{R} = \frac{1}{2}\left(\cos E + e, \sqrt{1-e^2}\sin E, 0\right)^{\mathrm{T}}.$$

Furthermore, we assume that the primaries are at their apocenter at $t = 0$.

The aim of this paper is to compute some families of 3D periodic orbits (PO) of the (ERTBP) as well as to locate transitions to complex instability, as a first step to analyze the dynamics around the transition to complex instability in this problem. More concretely, we show a way of generating families of PO, such that each family starts at a bifurcation orbit of a *limiting* Restricted Problem. By a limiting problem we mean the ERTBP with some restrictions; in particular, the Planar Isosceles Restricted Problem (PIRP) and the Sitnikov Problem (SP) are considered.

We begin with the PIRP: the two dimensional plane where the motion of the particle takes place is perpendicular to the line orbit of the primaries, which oscillate with consecutive Keplerian elliptic collisions (this problem is a limiting one of the ERTBP with the eccentricity of the orbit of the primaries e equals to 1, and the motion of the particle restricted to a plane). Puel (1979) studied some solutions (not periodic in the phase space) of this problem. We recover Puel's results from another point of view (see section 2) which allows us to obtain also new families not described there. Some isolated PO of the PIRP give rise to some families of the ERTBP (see section 3). This is done by means of a continuation method with respect to an eccentricity-like parameter. An analysis of the stability of the orbits computed reveals that there exist some transitions to complex instability as well as some critical orbits (with a stability parameter equal to -2 or 2, see Poincaré 1899 and section 3), which are candidates for bifurcation to other families of periodic orbits (with the same or double period).

On the other hand we analyze the Sitnikov Problem (see section 4). This is a special case of the 3D ERTBP. We assume that the particle moves on the axis perpendicular to the orbital plane of the two equally massive primaries, which move on Keplerian orbits around their common center of gravitation, that is, the ERTBP with e varying from 0 to 1, and the particle restricted to move on a line. Sitnikov (1960) gave the first qualitative results for some oscillatory motions and later Moser (1973), Llibre & Simó (1980) and Wodnar (1992) revisited them. Jie Liu & Yi-Sui Sun (1990) replaced the differential equations by a mapping and derived the existence of an hyperbolic invariant set. Hagel (1992) and Hagel & Trenkler (1993) carried out an analytical approach for bounded small amplitude solutions. Martinez & Chiralt (1997) proved the existence of invariant curves close to the origin for a sequence of values of the eccentricity in $[0, 1]$. From a numerical point of view, Dvorak (1993) showed the great variety of possible orbits in this problem in the range $0.33 \leq e \leq 0.66$. For the limiting case $e = 1$, Broucke (1971, 1979) classified some periodic orbits depending on the number of ascending and descending segments (arcs) in a revolution; in Waldvogel (1973) asymptotic expansions of a solution near a triple collision and during a parabolic and hyperbolic escape were derived. Later Martinez & Orellana (1997) and Álvarez (1997) analyzed exhaustively the distribution of the regions of bounded, hyperbolic and collision orbits and obtained some results on collision and final evolution orbits according to the crossings with the line described by the primaries. The other limiting case, $e = 0$, the so called MacMillan Problem, was originally discussed by MacMillan (1913) who showed that this problem is integrable using elliptic integrals; later revisited in Belbruno et al. (1994) where, in fact, periodic orbits of the MacMillan problem are regarded as particular orbits of the Circular Spatial RTBP in order to generate families of periodic orbits of the RTBP. And, precisely, this is the point of view taken in this paper. We consider the Sitnikov problem as a particular case of the ERTBP. We start with the limiting cases $e = 1$ and $e = 0$, and we compute the families of periodic orbits for varying $e \in [0, 1]$ and their stability. Actually, these orbits are highly unstable, transitions to complex instability do exist and critical periodic orbits which bifurcate again to periodic orbits of the SP are also given. Finally, in section 5 we draw some conclusions.

2. The Planar Isosceles Restricted Problem

Let us consider two primaries with equal masses, moving along a fixed axis in a degenerate elliptic periodic orbit with eccentricity equal to one, whilst the test particle moves in the perpendicular invariant plane which contains the center of mass of the two primaries. We denote R and θ the polar coordinates of the particle in the plane of symmetry (see Fig. 1) and in the inertial system described in the introduction, the equations of motion of the particle are

$$\begin{aligned}
\frac{\mathrm{d}R}{\mathrm{d}E} &= (1+\cos E)\,\dot{R}, \\
\frac{\mathrm{d}\dot{R}}{\mathrm{d}E} &= (1+\cos E)\left\{\frac{-R}{\left[R^2+\frac{1}{4}(1+\cos E)^2\right]^{\frac{3}{2}}}+\frac{C^2}{R^3}\right\}, \\
\frac{\mathrm{d}\theta}{\mathrm{d}E} &= (1+\cos E)\,\frac{C}{R^2},
\end{aligned} \tag{2}$$

where C is the area constant of the particle and the dot denotes the derivative with respect to the time t.

The above equations have been studied by Puel (1979), who obtained families of symmetric periodic orbits *only* in the $(R, \dot{R})$ phase plane. That is, since the two first equations in the system (2) are decoupled with respect to the third one, both may be taken as the Hamiltonian equations whose non

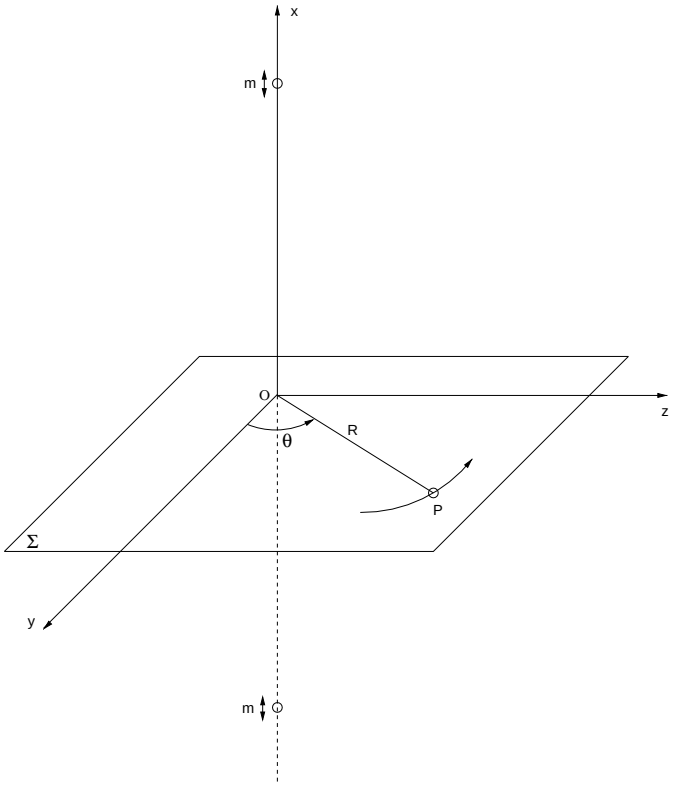

Fig. 1. The Planar Isosceles Restricted Problem (PIRP). The particle P moves on the invariant plane $\Sigma = \{(x, y, z) : x = 0\}$, while the two primaries oscillate along the x-axis.

autonomous Hamiltonian function with one degree of freedom is,

$$H = \cos^2 \frac{E}{2} \left\{ \dot{R}^2 + \frac{-2}{\left[R^2 + \frac{1}{4}\left(1 + \cos E\right)^2\right]^{\frac{1}{2}}} + \frac{C^2}{R^2} \right\}, \quad (3)$$

and then one can study the dynamical backbone of the Hamiltonian system (3) by itself without any reference to the third equation in (2). So, from now on, we will only consider equations (2a) and (2b). Later on, when we shall look for periodic orbits in the configuration space, the third equation will be explicitly taken into account.

2.1. The central family of periodic orbits

Let $R\left(R_0, \dot{R}_0, C; E\right)$, $\dot{R}\left(R_0, \dot{R}_0, C; E\right)$ be a solution of equations (2a), (2b), with initial conditions R_0, $\dot{R}_0 = 0$, for $E = 0$. Equations of motion (2a), (2b) have the following symmetry

$$\left(R, \dot{R}, E\right) \mapsto \left(R, -\dot{R}, -E\right),$$

thus, given a fixed value of C, if R_0 satisfies

$$\dot{R}\left(R_0, 0, C; m\pi\right) = 0, \quad (4)$$

for $m \in \mathbb{N}$, then we obtain a periodic orbit of period $2m\pi$ which is symmetric with respect to the R axis, with initial conditions R_0, $\dot{R}_0$, for $E = 0$.

In order to have a first approximation of a periodic orbit we remark that if $R \gg 1$ equations (2a), and (2b) can be approximated by

$$\begin{aligned} \frac{\mathrm{d}R}{\mathrm{d}E} &= \left(1 + \cos E\right) \dot{R}, \\ \frac{\mathrm{d}\dot{R}}{\mathrm{d}E} &= \left(1 + \cos E\right) \left(-\frac{1}{R^2} + \frac{C^2}{R^3}\right), \end{aligned}$$

so we consider the constant solution,

$$R = C^2, \quad \dot{R} = 0,$$

for C large enough. Then $R \gg 1$, and this orbit will be close to a 2π-periodic orbit of equations (2a), (2b). Once this first approximation is refined and one periodic orbit of the system (2a), (2b) is known for some large value of C, we continue this periodic solution with respect to the parameter C. In fact, we fix $m = 1$, and we look for a curve $(R_0(s), C(s))$, satisfying equation (4),

$$\dot{R}\left(R_0(s), 0, C(s), \pi\right) = 0,$$

being s the arc length parameter. The numerical method used consists in finding the continuation curve as the solution of a differential system of equations; therefore, we use an Adams-Bashforth method of order 4 to predict a new point on the continuation curve, and a modified Newton method to refine it (see Gómez et al. 1985; Belbruno et al. 1994 for details). We have called Central Periodic Orbits (CPO) the orbits of period 2π obtained and we show this family in Fig. 3.

2.2. Bifurcation branches

Actually, central periodic orbits can also be regarded as periodic orbit of period $2m\pi$, $m \in \mathbb{N}$, and therefore, their initial conditions satisfy equation (4).

The continuation procedure we have just described breaks down when the quantity,

$$G_m := \left(\partial_{R_0} \dot{R}\left(R_0, C; m\pi\right)\right)^2 + \left(\partial_C \dot{R}\left(R_0, C; m\pi\right)\right)^2, \quad (5)$$

(where we take $\dot{R}_0 = 0$), is equal to zero; and it is related to the appearance of bifurcations of periodic orbits of period $2m\pi$ (see details in Pacha 1999). In our case, when $m = 1$ is taken, no bifurcations appear. But this is not so for higher values of m. For example, for $m = 5$, the value of the above defined function G_5 is plotted with respect to C (see Fig. 2).

Varying m from 1 to 6, several multiple period families bifurcating from the family of CPO have been found. We have labeled the bifurcating branches as B_m^n, where $m\pi$ is the half period of the orbits in the family, and n denotes the ordinal number of the family in relation to those with the same period. In the same way, these branches which bifurcate from the CPO, may in turn undergo bifurcations. This is the case for the family

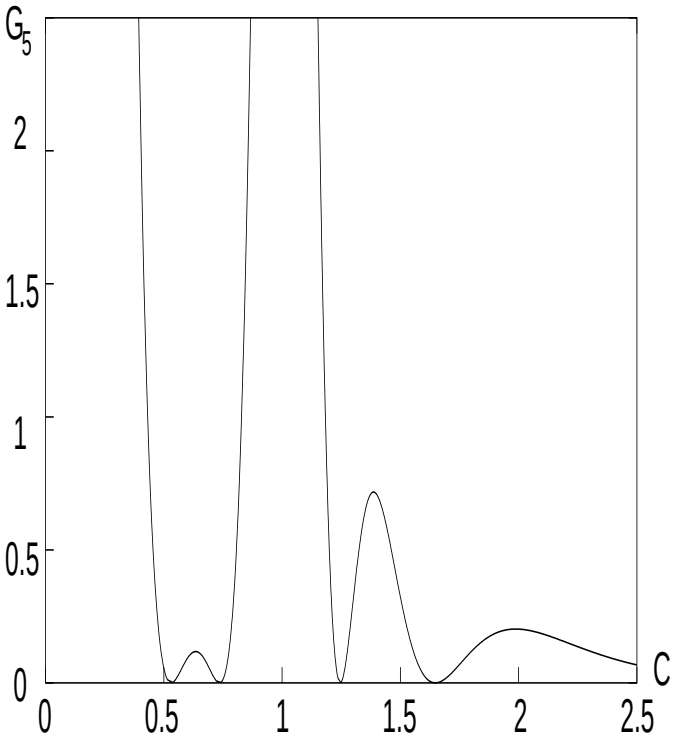

Fig. 2. Projection of the function $G_5(R_0, C)$ on the C axis. In the range of C and R_0 explored, four zeroes of the function G_5 have been found, so the same number of branches with period 10π are expected to bifurcate.

Table 1. Bifurcation points in the C–R_0 continuation diagram. B_m^n stands for branches of $2m\pi$ periodic orbits which bifurcate from the CPO, while C_m^n stands for bifurcated branches of the B_2^1 family.

Branch	C	R_0	Located in
B_2^1	1.1765511346934	1.7487386405564	CPO
B_3^1	1.3426927497254	2.1418415988432	CPO
B_4^1	1.5102062188830	2.5856660387275	CPO
B_5^1	0.5308000682332	0.5594663779554	CPO
B_5^2	0.7352859719827	0.8615662980553	CPO
B_5^3	1.2459732416503	1.9079499265106	CPO
B_5^4	1.6476574740433	2.9906156603910	CPO
B_6^1	1.7650033649783	3.3671870541442	CPO
C_4^1	1.0452073096396	2.2865552234104	B_2^1
C_6^1	1.0841417333407	2.2042022799551	B_2^1
C_6^2	1.0841417333407	1.2651031672737	B_2^1

B_2^1, which presents three branches: two with $m = 6$, and one with $m = 4$. These secondary bifurcations have been labeled in the same way, but using the letter C, i.e.: C_6^1, C_6^2, C_4^1.

For all the orbits obtained, we have computed the trace of the monodromy matrix which describes their stability behavior (see Fig. 3). Finally, we give the initial conditions of the bifurcating orbits of every one of the continuation branches in Table 1.

Table 2. Values of the initial condition $R_0 = z_0$ when $C = 0$ for the limiting orbits of the families which do not end in triple collision. We notice the duplication of the period

Limiting orbit	R_0 at $C = 0$	Period
SB_2^1	2.926182494668	8π
SC_4^1	3.418502434838	16π
SB_4^1	4.858835984845	16π
SB_6^1	6.452096441956	24π

2.2.1. Remarks

1. We used the symmetry of the equations (2a), (2b) to reduce both the number of equations to integrate numerically and the time interval over which they must be integrated (just a half period is enough: see Katsiaris 1973).
2. The family of CPO may be also obtained taking as approximations the circular (*first kind*) orbits of the two body problem when $R_0 \gg 1$, whose initial conditions are given by the parabola $R_0 = C^2$. Similarly, the bifurcating branches B_m^n can be approximated, if $R_0 \gg 1$, by the elliptic (*second kind*) orbits, whose initial conditions satisfy the equation $kT = 2\pi m$ ($k, m \in \mathbb{N}$ and T the period of the particle), or equivalently they belong to the ellipses

$$\frac{R_0^2}{2R_0 - C^2} = \left(\frac{m}{k}\right)^{2/3}.$$

   This was the point of view taken in Puel's (1979), but not here. We point out that our approach allows to find *all* the branching families. In particular, we note that the branching families B_5^1 and B_5^2 in Fig. 3 do not appear in Puel's paper.
3. We also remark that all the families B_m^n end at the Lagrangian equilibrium point L_1 ($R = 0$, $\dot{R} = 0$) or at the periodic orbit of the *Rectilinear* Isosceles Restricted Problem ($C = 0$). Since they were not studied in Puel's paper, and they will play their role to compute periodic orbits of the ERTBP (see section 4), we describe them in the next subsection.

2.3. Limiting periodic orbits when $C \to 0$

When the decreasing parameter C is equal to zero, the particle does no more move in a plane, but in a line, that is, we have the Rectilinear Isosceles Restricted Problem (RIRP). So branching families B_m^n are born at the family of CPO, and end in a periodic orbit of the RIRP (except B_5^1 and B_5^2, which finish in the Lagrangian point L_1).

Since, when $C = 0$ the particle moves in the z-axis ($\theta = \pi/2$, constant), we replace R and $\dot{R}$ with z and $\dot{z}$. Of course, a periodic orbit of period T in R and $\dot{R}$ becomes a periodic orbit of period $2T$ in z and $\dot{z}$.

Two different kinds of limiting orbits have been found: either *regular* (not collision) or triple collision periodic orbits of the RIRP. On one hand, families B_2^1, C_4^1, B_4^1 and B_6^1 end at *regular* orbits: we call them SB_2^1, SC_4^1, SB_4^1 and SB_6^1 respectively. We give their corresponding values of R_0 at table 2, and plot

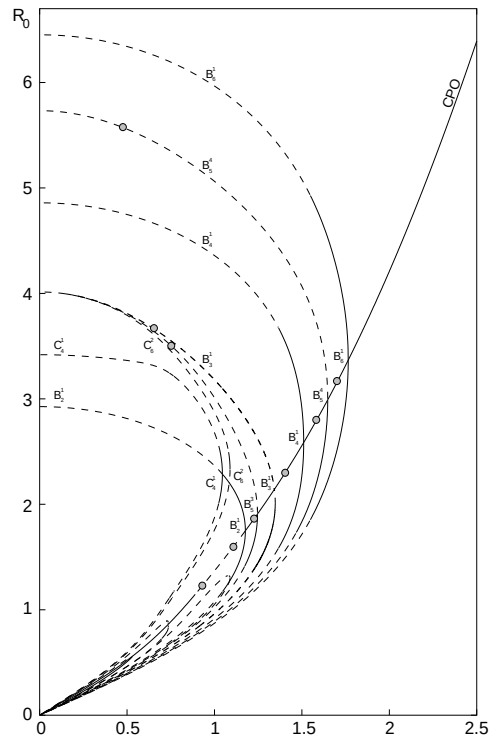

Fig. 3a.

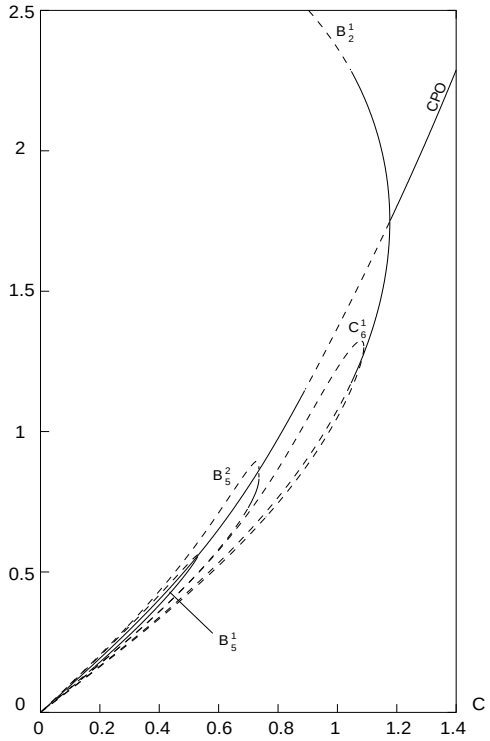

Fig. 3b.

Fig. 3. a initial conditions of symmetric periodic orbits. The stable ones belong to the full line, while dashed lines represent the unstable ones. Periodic orbits in the configuration space are marked with bullets (∘). **b** detail for low values of C and R_0. More precisely, families B_5^1, B_5^2, C_6^1, B_2^1, and the CPO. The other ones have been omitted for the sake of clarity.

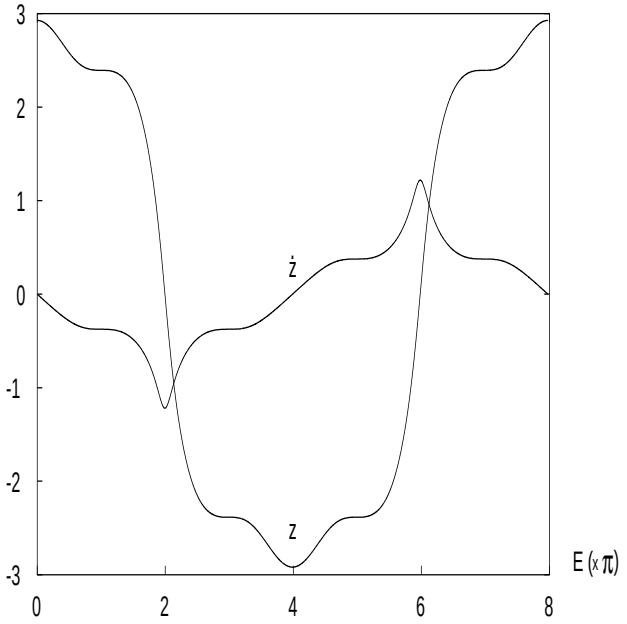

Fig. 4. Final orbit ($C = 0$) of the family B_2^1. We plot z and $\dot{z}$ as functions of the eccentric anomaly of the primaries, E.

one of them in Fig. 4 (where z and $\dot{z}$ are plotted as functions of E).

On the other hand, as Fig. 3 shows, families B_3^1, B_5^3 and C_6^2 tend to the same final orbit, we call it SCOL_3, as C goes to zero. It turns out to be a solution with a triple collision at $E = 3\pi$, as can be seen in Fig. 5a, where the z variable of the particle at $E = 3\pi$ is plotted when decreasing C. In Fig. 5b, the same is done with the family B_5^4; but in this case, the triple collision with the primaries takes place at $E = 5\pi$, so the value of z is plotted at this time for every periodic orbit, when varying C.

By a kind of bisection method, we computed the initial conditions of those two triple collision orbits: $z_0 = 4.013570495$, $\dot{z} = 0$, for the limiting orbit SCOL_3, and $z_0 = 5.732495298$, $\dot{z} = 0$ for the limiting orbit SCOL_5 of family B_5^4.

2.3.1. Remarks

1. Álvarez (1997) and Martinez & Orellana (1997) analyzed the global flow of the RIRP and, in particular, they studied triple collision orbits. Although they did not compute them numerically, they gave some results according to the number of crossings with the section $z = 0$ and the number of binary collisions between the primaries. In fact, following ideas in Álvarez (1997) – a numerical method which consists of computing the intersection between the invariant manifolds of the equilibrium points in the collision manifold, and the section $\dot{z} = 0$ –, the initial conditions of the triple collisions given above might also be computed.
2. We identify the regular limiting orbits computed above with those found by Broucke (1979), where he classified periodic orbits with different number of arcs (related to crossings with $z = 0$).

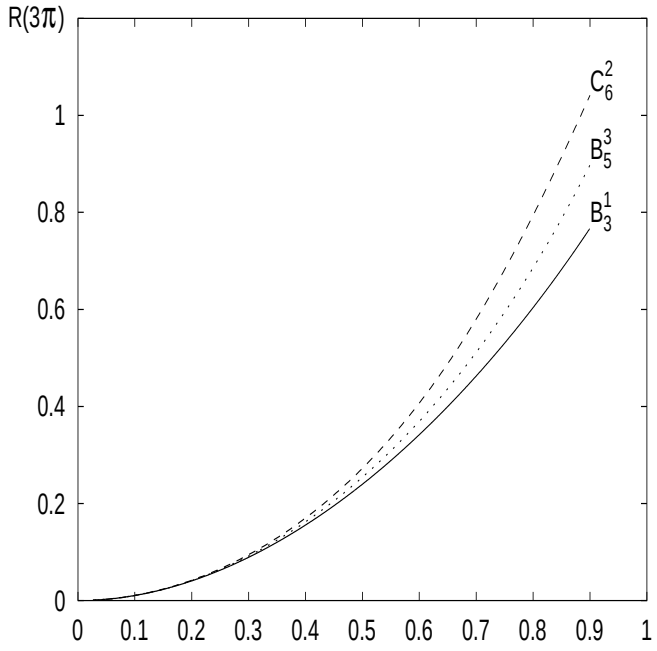

Fig. 5a.

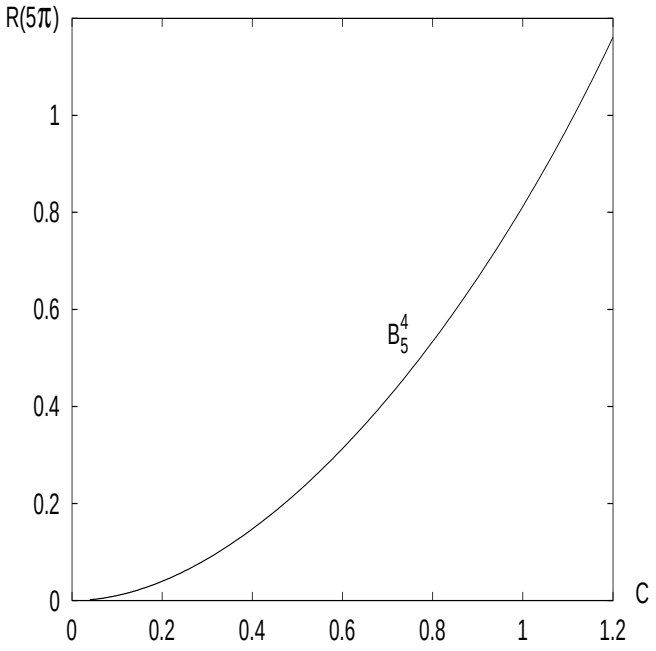

Fig. 5b.

Fig. 5. Final orbits of families ending at triple collision trajectories. **a** values of R at $E = 3\pi$ when decreasing C for the families B_3^1, B_5^3 and C_6^2. **b** R at $E = 5\pi$ for each orbit of the family B_5^4.

Table 3. Values of C and R_0 of the isolated periodic orbits $\mathrm{O}_{m\nu}^l$ of the PIRP. The last column indicates the family of radial oscillations which the PO belongs to.

l	m	ν	C	R_0	Branch
1	2	0	0.922561907659	1.211183397095	CPO
1	3	0	1.238438876233	1.890342460648	CPO
1	4	0	1.434785790400	2.379377210675	CPO
1	5	0	1.587450132530	2.808521427743	CPO
2	5	0	1.108995026782	1.599696028138	CPO
1	6	0	1.714676035963	3.202143058164	CPO
1	3	1	0.628958992581	3.689815429837	B_3^1
1	5	1	0.488634028936	5.564719773691	B_5^1
2	5	1	0.743985689857	3.516672684922	B_5^2

2.4. Periodic orbits in the configuration space

In the previous section, several families of symmetric periodic orbits have been determined in the $(R, \dot{R})$ plane. But these are actually only radial oscillations of the particle. Since we look for periodic orbits of the Elliptic RTBP which bifurcate from the Isosceles Restricted Problem, we need periodic orbits in the configuration space (R, θ) that we call *real* periodic orbits. Thus we want to check out if, among the orbits computed, periodic solutions of the whole system (2) do exist. That is, we look for values (R_0, C) which fulfill simultaneously the two equations,

$$\begin{aligned} \dot{R}\,(R_0, 0, 0, C; m\pi) &= 0, \\ \theta\,(R_0, 0, 0, C; m\pi) - l\pi &= 0, \end{aligned}$$

$l, m \in \mathbb{N}$. Taking into account that the points in the bifurcation diagram of Fig. 3 satisfy – for their corresponding m –, the first equation, only changes of sign in the second equation must to be detected. Varying m and l from 1 to 6, we have obtained the isolated symmetric periodic orbits given in Table 3. We have labeled such orbits as $\mathrm{O}_{m\nu}^l$, since the particle needs l revolutions around the origin in m periods of the primaries before going back to its original position in the YZ plane (see Fig. 1); ν is a dichotomic parameter whose value is equal to 0 if the orbit belongs to the CPO family or 1 otherwise. These "real" periodic orbits are marked in Fig. 3 with bullets ($\circ$).

Thus, we have six periodic orbits on the CPO family: O_{20}^1, O_{30}^1, O_{40}^1, O_{50}^1, O_{60}^1 and O_{50}^2 plus three additional orbits, O_{31}^1, O_{51}^1, O_{51}^2 on the branches B_3^1, B_5^1 and B_5^2, respectively. These orbits are plotted in Fig. 6.

In relation to our main goal of obtaining families of periodic orbits of the ERTBP for any value of the eccentricity $e \in [0, 1]$, and also transitions to complex instability, we may conclude from our computations that the natural candidates of families of periodic orbits of the ERTBP start at:

1. The *real* periodic orbits of the Planar Isosceles Restricted Problem (this is done in the next section) and,
2. The periodic orbits of the RIRP ($C = 0$ and $e = 1$). We follow them in the Sitnikov Problem when varying the eccentricity from 1 to 0. The critical orbits in these families may also bifurcate to families of periodic orbits of the ERTBP (see section 4).

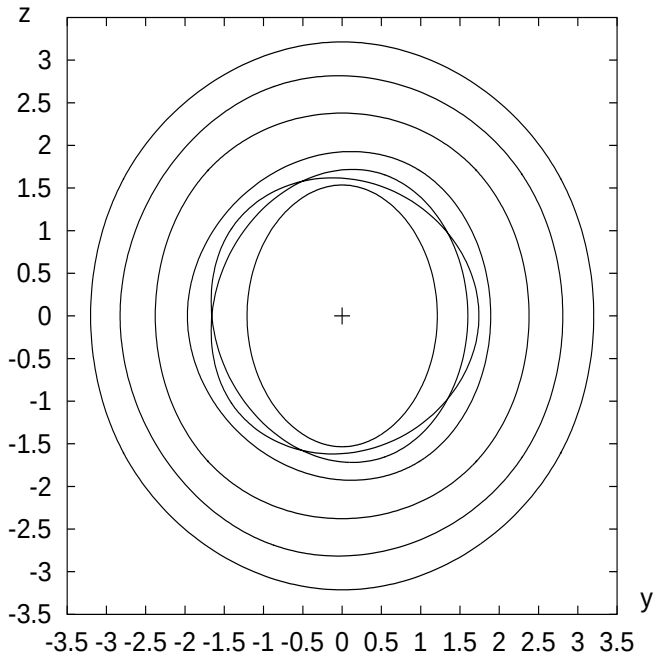

Fig. 6a.

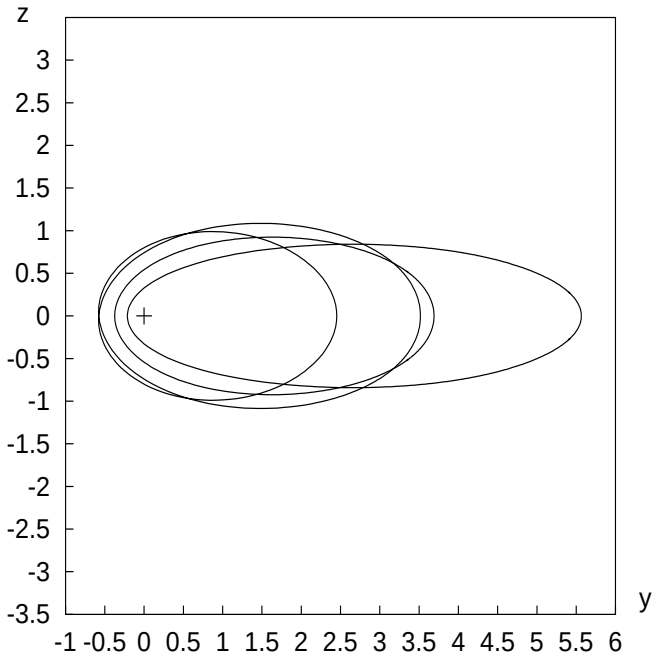

Fig. 6b.

Fig. 6. a real periodic orbits of the PIRP on the CPO. Going from inner to outer: O^1_{20}, O^2_{50} (double looped), O^1_{30}, O^1_{40}, O^1_{50}, O^1_{60} and **b** real periodic orbits on the bifurcation branches (see table 3). These are, in increasing order of amplitudes: O^2_{51} (double looped), O^1_{31}, O^1_{51}.

3. The Spatial Elliptic Restricted Three-Body Problem with equal masses

3.1. Equations of motion. Periodic orbits

We now consider the general problem, the Elliptic Restricted Three Body Problem with equal masses. As stated in the introduction, the motion of the particle in the inertial frame of coordinates, is described by the Hamiltonian equations which come from the Hamiltonian function (1). These are, written in vectorial notation,

$$\begin{aligned} \frac{\mathrm{d}\boldsymbol{\xi}}{\mathrm{d}E} &= (1+e\cos E)\,\boldsymbol{\eta}, \\ \frac{\mathrm{d}\boldsymbol{\eta}}{\mathrm{d}E} &= -\frac{1}{2}(1+e\cos E)\left(\frac{\boldsymbol{\sigma}_1}{\|\boldsymbol{\sigma}_1\|^3}+\frac{\boldsymbol{\sigma}_2}{\|\boldsymbol{\sigma}_2\|^3}\right). \end{aligned} \tag{6}$$

As stated before, $\boldsymbol{\xi}$ and $\boldsymbol{\eta}$ are the position and the velocity respectively, while $\boldsymbol{\sigma}_1$, $\boldsymbol{\sigma}_2$ stands for the positions of the particle with respect to the primaries (see Fig. 7).

The orbits obtained in section 2.4 are in fact solutions of (6) for the eccentricity $e = 1$ and the initial conditions,

$$\begin{aligned} &x_1^0 = 0, \quad x_2^0 = R_0, \quad x_3^0 = 0, \\ &x_4^0 = 0, \quad x_5^0 = 0, \quad x_6^0 = \frac{C}{R_0}. \end{aligned} \tag{7}$$

On the other hand, it is well known (see Macris et al. 1975), that a solution $\boldsymbol{\xi}\left(\boldsymbol{\xi}^0, \boldsymbol{\eta}^0, e; E\right), \boldsymbol{\eta}\left(\boldsymbol{\xi}^0, \boldsymbol{\eta}^0, e; E\right)$ of (6) with initial conditions

$$x_1^0 = x_3^0 = x_5^0 = 0, \tag{8}$$

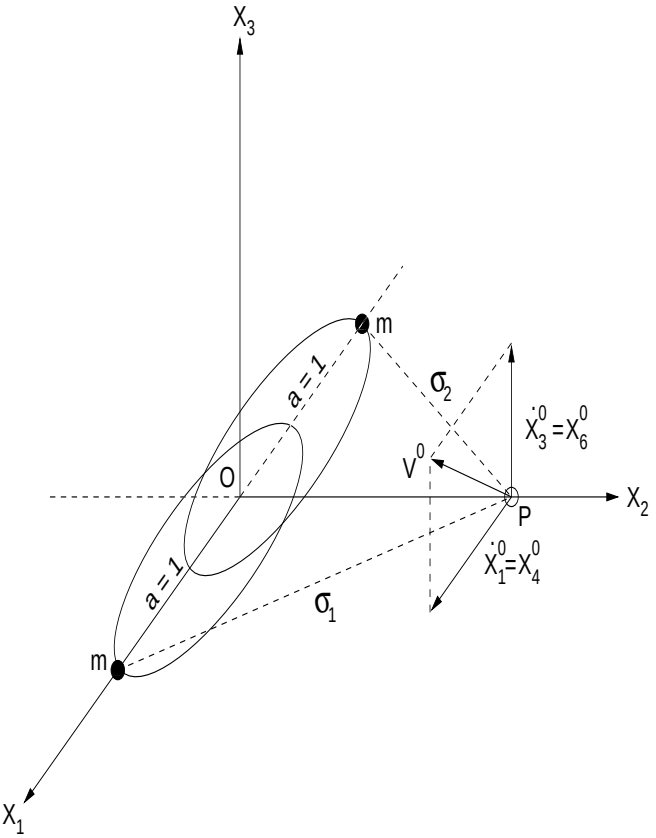

Fig. 7. The Spatial Elliptic Restricted Three Body Problem with equal masses on an inertial (non rotating) system of coordinates.

and such that

$$\begin{aligned} x_1\left(0,x_2^0,0,x_4^0,0,x_6^0,e;p\pi\right) &= 0,\\ x_3\left(0,x_2^0,0,x_4^0,0,x_6^0,e;p\pi\right) &= 0,\\ x_5\left(0,x_2^0,0,x_4^0,0,x_6^0,e;p\pi\right) &= 0, \end{aligned} \tag{9}$$

is a periodic orbit of period $2\pi p$ and symmetric with respect to the y-axis. Therefore, we can continue the obtained periodic orbits – for $e=1$ and initial conditions given by (7) – with respect to the parameter e, in order to have symmetric periodic orbits of the ERTBP.

The continuation method with the arc parameter quoted in section 2 is also applied. At this point, we have to mention that the right hand side of the equations (6) are not regular in the eccentricity e at $e=1$, for the partial derivatives of the field with respect to e, are not defined for $e=1$. Therefore the derivatives

$$\frac{\partial x_i}{\partial e}\left(0,R_0,0,0,0,\frac{C}{R_0},1;p\pi\right),$$

for $i=1,3,5$ cannot be computed from the variational equations of the system (6). To skip this lack of regularity we have changed the parameter e and introduced a new "eccentricity-like" parameter, p, defined by $p:=\sqrt{1-e^2}$. The equations (6) are then replaced by the following ones, which we write down explicitly,

$$\begin{aligned} \frac{\mathrm{d}x_1}{\mathrm{d}E} &= \left(1+\sqrt{1-p^2}\cos E\right)x_4,\\ \frac{\mathrm{d}x_2}{\mathrm{d}E} &= \left(1+\sqrt{1-p^2}\cos E\right)x_5,\\ \frac{\mathrm{d}x_3}{\mathrm{d}E} &= \left(1+\sqrt{1-p^2}\cos E\right)x_6,\\ \frac{\mathrm{d}x_4}{\mathrm{d}E} &= \frac{\left(1+\sqrt{1-p^2}\cos E\right)}{4}\left\{\frac{\cos E+\sqrt{1-p^2}-2x_1}{\|\boldsymbol{\sigma}_1\|^3}\right.\\ &\quad\left.-\frac{\cos E+\sqrt{1-p^2}+2x_1}{\|\boldsymbol{\sigma}_2\|^3}\right\},\\ \frac{\mathrm{d}x_5}{\mathrm{d}E} &= \frac{\left(1+\sqrt{1-p^2}\cos E\right)}{4}\left\{\frac{p\sin E-2x_2}{\|\boldsymbol{\sigma}_1\|^3}\right.\\ &\quad\left.-\frac{p\sin E+2x_2}{\|\boldsymbol{\sigma}_2\|^3}\right\},\\ \frac{\mathrm{d}x_6}{\mathrm{d}E} &= \frac{\left(1+\sqrt{1-p^2}\cos E\right)}{2}\left\{\frac{-1}{\|\boldsymbol{\sigma}_1\|^3}+\frac{-1}{\|\boldsymbol{\sigma}_2\|^3}\right\}x_3, \end{aligned} \tag{10}$$

now with,

$$\begin{aligned} \boldsymbol{\sigma}_1 &= \left(x_1-\frac{\cos E+\sqrt{1-p^2}}{2},x_2-\frac{p\sin E}{2},x_3\right),\\ \boldsymbol{\sigma}_2 &= \left(x_1+\frac{\cos E+\sqrt{1-p^2}}{2},x_2+\frac{p\sin E}{2},x_3\right). \end{aligned}$$

We have continued all the periodic orbits in the Table 3, generating thus families of periodic orbits in the ERTBP and we have studied their stability (integrating the variational equations together with the ones of motion). Each family is identified with the label $\mathrm{F}^l_{m\nu}$, since it starts at $p=0$ (that is $e=1$), at the orbit $\mathrm{O}^l_{m\nu}$ from the Rectilinear Isosceles Restricted Problem.

3.2. Description of families $\mathrm{F}^l_{m\nu}$. Stability

It is well known that the linear stability of a periodic orbit depends on the eigenvalues of its monodromy matrix. Since (10) is a Hamiltonian system, the monodromy matrix is symplectic and its eigenvalues come in reciprocal pairs: λ_i, $1/\lambda_i$, for $i=1,2,3$. The stability parameters are defined by

$$b_i=-\left(\lambda_i+\frac{1}{\lambda_i}\right),$$

also for $i=1,2,3$; and we refer the reader to Broucke (1969) and Katsiaris (1973) for a detailed explanation on how to compute the linear stability from them. Here, we only recall that a periodic orbit is *stable* (S), if the three parameters b_i are in the interval $(-2,2)$, *unstable* (U), if at least one stability parameter b_i satisfies $|b_i|>2$, and finally, if one parameter is real and the remaining b_i, b_j are complex, then the orbit is *complex unstable* (Δ). If, following Pfenniger (1985a), we define

$$\Delta:=(b_i-b_j)^2,$$

then, for complex unstable orbits, we have $\Delta<0$, and it is usual to replace the complex parameters b_i, b_j (see Pfenniger, 1985a) by

$$\begin{aligned} c_i &= \frac{1}{2}\left(b_i+b_j\right),\\ c_j &= \frac{1}{2}\left|\Delta\right|^{1/2}. \end{aligned}$$

We also remark that any *critical* periodic orbit with period T, with a stability parameter equal to -2 or 2 is a candidate to give bifurcating families of periodic orbits of period T or $2T$ respectively. In the same way, when four eigenvalues collide simultaneously by conjugate pairs on the unit circle and leave it in the complex plane, then there bifurcate multiple periodic orbits or invariant 2D tori if the transition point on the unit circle corresponds to an angle that is rational or irrational with respect 2π, respectively. Of course this last case is the generic one, but there are examples of multiple period bifurcating orbits for the *rational* transition to Δ in the circular 3D RTBP (see Ollé & Pacha, 1998).

When computing families $\mathrm{F}^l_{m\nu}$ as continuation of the periodic orbits of the Isosceles Problem, three different behaviors have been detected (see from Fig. 9 to Fig. 16).

1. Families $\mathrm{F}^l_{m\nu}$ with $\nu=0$ – starting at CPO –, $l=1$ and m ranging form 2 to 6 reach $p=1$ ($e=0$), that is, each one of these families ends in a periodic orbit of the Spatial *Circular* Restricted Problem. Their characteristic curves are plotted from Fig. 9 to 13. In these figures, the stable orbits of the families are drawn in continuous lines, the unstable

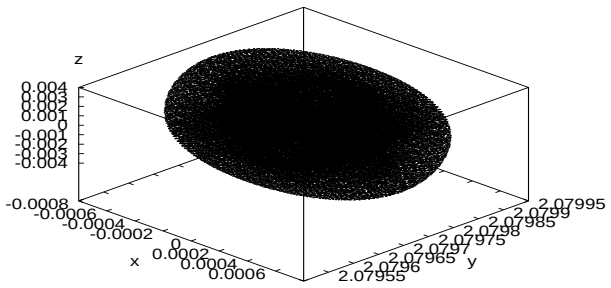

Fig. 8a.

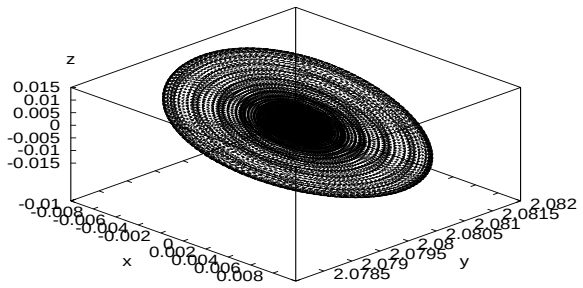

Fig. 8b.

Fig. 8. 100000 iterates of the time-fixed map generated by the flow and with $E = 6\pi$. In **a** the initial conditions are taken close to the stable orbit of the family F^1_{30} with $p = 0.9999722$. In **b** we choose initial conditions near a complex unstable orbit with $p = 0.9999712$.

ones in dashed lines and the complex-unstable regions are plotted with dotted lines. From their stability parameters, we conclude that the family F^1_{20} has four critical orbits: actually, apart from the tangency with $b_2 = -2$ at $p = 0$, there are two more tangencies, with $b_1 = 2$, at $p = 0.7376$ and at $p = 0.9353$. The other two critical orbits correspond to $p = 0.9778$ and $p = 0.9975$, where the index b_2 crosses the line $b_2 = -2$, decreasing for the former value of p and increasing for the later (both crossings are too close to $p = 1$ and cannot be appreciated at Fig. 9b). All the orbits in this family are unstable (see Fig. 9a). Family F^1_{30} has one critical orbit (for $p = 0.9814$ the index b_3 crosses the value $b_3 = -2$), and four transitions to complex instability (Δ), that is, two complex-unstable intervals (see Fig. 10a): for $p \in (0.0148, 0.8206)$ and for $p \in (0.9936, 0.9999)$. In particular, as stated above, there will bifurcate 2D tori from three of them (the first two ones with $p < 0.9$ and the closest to the end, at $p = 0.9999715$). In this last transition to complex instability, as the third stability index (b_1 in Fig. 10) is less than two in absolute value, the flow around the unstable orbit will remain confined if furthermore the bifurcation is of direct type. Actually, this is so. Fig. 8a and b display several iterates of the fixed-time map. In Fig. 8a, for initial conditions close to an stable orbit; as can be guessed from the figure, the flow is bound to fill densely a 4D torus in the extended phase space (i.e., adding E and the Hamiltonian H as its conjugated variable). This family of big relative measure tori, appears together with lower dimensional tori, which come from resonances among the different intrinsic frequencies (see Jorba & Villanueva 1997). On the other hand, in Fig. 8b, the initial conditions are taken near a complex-unstable orbit. A region of strong confinement for a long time – due to the stable and unstable manifolds of the complex-unstable orbit –, can be appreciated. At this point, we mention that the iterates plotted in Fig. 8 should be close to the iterates of the invariant manifolds of the unstable orbit (manifolds of this type have been obtained, for a Hamiltonian of a galactic model in Papadaki et al. 1995). In such domain, 2D stable tori, surrounded by 3D ones, are expected to bifurcate (see Bridges et al. 1995; Heggie 1985 and Jorba & Villanueva 1997).

2. Family F^1_{40} has most stable orbits and three critical orbits (see Fig. 11).
3. Family F^1_{50} has two transitions from stability to Δ. The first at $p = 0.6311765$ and the second at $p = 0.9798355$, both give rise to other bifurcations of the same type as the one described above for the family F^1_{30} (see Fig. 8). Furthermore, this family is somewhat special, in the sense that the index b_1 is extremely close – specially for small p – to the critical value -2 (see Fig. 12), e.g., even for $p = 0.5$, we have $b_1 = -1.9999991$.
4. Family F^1_{60} behaves as the previous one, but without transitions to Δ. Its characteristic diagram and its stability indices in front of p are plotted in Fig. 13.
5. Families F^2_{50} and F^2_{51} become actually the *same* family: the family generated by O^2_{50} ends at the orbit O^2_{51}, indeed again at $p = 0$. And conversely, the family we get by continuation from the orbit O^2_{51} does not reach $p = 1$, but turns back and ends at the orbit O^2_{50} (see Fig. 14a). It has four transitions to Δ. More precisely: a thin complex-unstable interval for $p \in (0.3221, 0.3257)$ and another one for $p \in (0.7107, 0.8176)$, before the family reaches its turning point and comes back to $p = 0$. The first complex-unstable interval is not seen in Fig. 14a, but its position is marked in Fig. 14c with a segment ($\backslash$). From Fig. 14c – a magnification of Fig. 14b –, eight critical orbits can be identified.
6. Families F^1_{31} and F^1_{51} do not reach $p = 1$. Instead, both families turn back, but now they end at two different orbits of the Rectilinear Isosceles Problem (Sitnikov Problem with $e = 1$). More concretely, they end at the triple collision orbits SCOL_3 and SCOL_5 respectively. See Fig. 15 and Fig. 16.

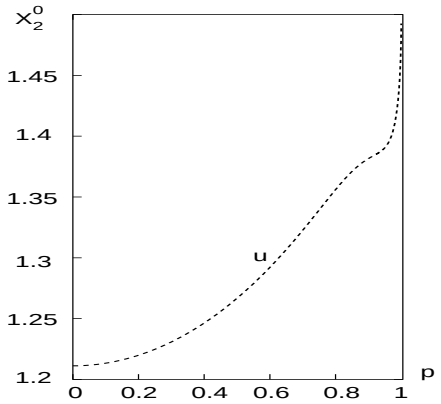

Fig. 9a.

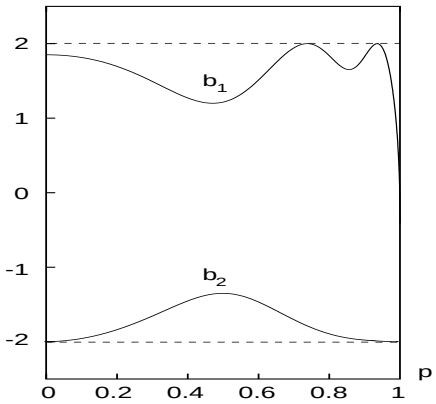

Fig. 9b.

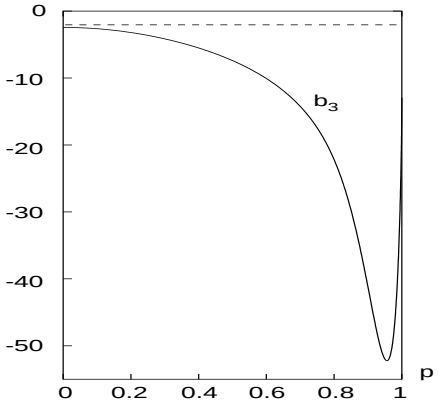

Fig. 9c.

Fig. 9. In **a**, the characteristic curve of the family F_{20}^1 is shown. We plot the initial condition x_2^0 v.s. p. The family reaches $p = 1$ ($e = 0$), so it ends in an orbit of the Spatial *Circular* Restricted Problem. In the figures **b** and **c** the stability indices b_1, b_2 and b_3 are plotted with respect to p. The third index, b_3, in the figure **c** is always less than -2. So all orbits in this family are unstable.

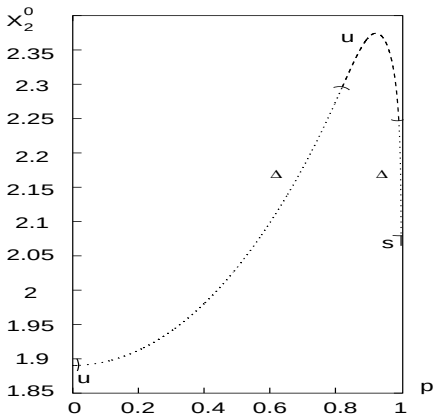

Fig. 10a.

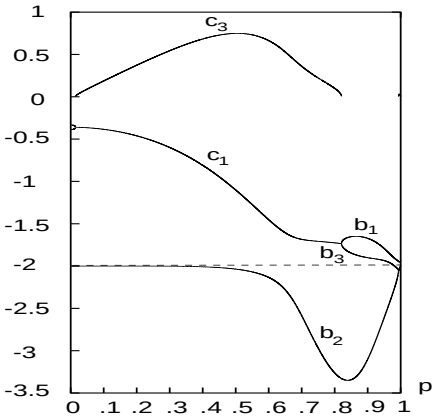

Fig. 10b.

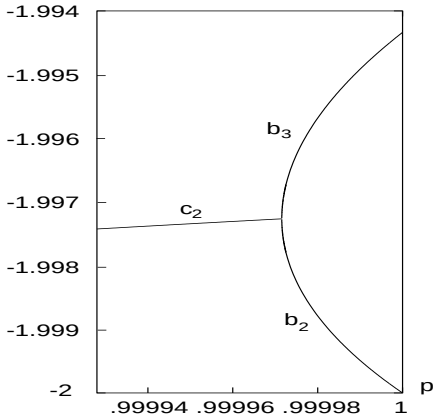

Fig. 10c.

Fig. 10. Family F_{30}^1. There are four transitions to complex instability, Δ. In particular, the last one, – which takes place at $p = 0.9999715$ –, is visible in **c**, which is a magnification of **b** for values of p very close to 1.

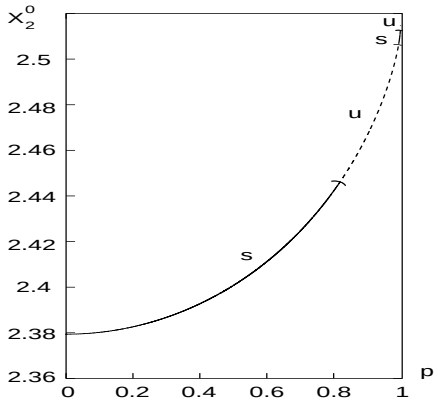

Fig. 11a.

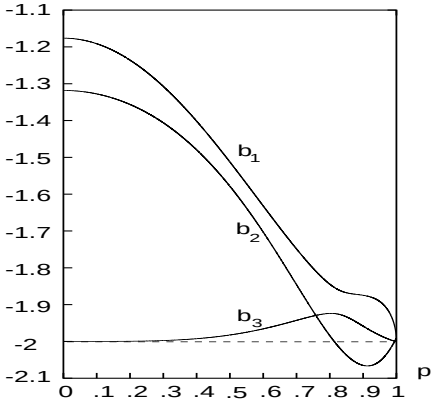

Fig. 11b.

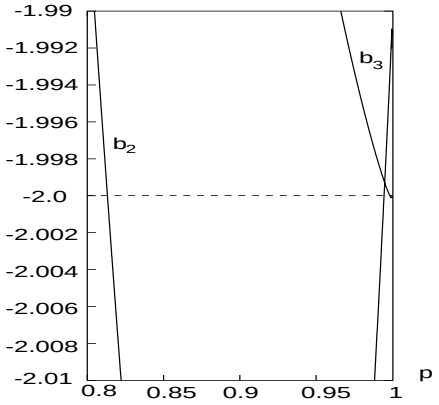

Fig. 11c.

Fig. 11. Family F_{40}^1. Most orbits in this family are stable. In figure **c** – a magnification of **b** –, we see three critical orbits from the stability curves.

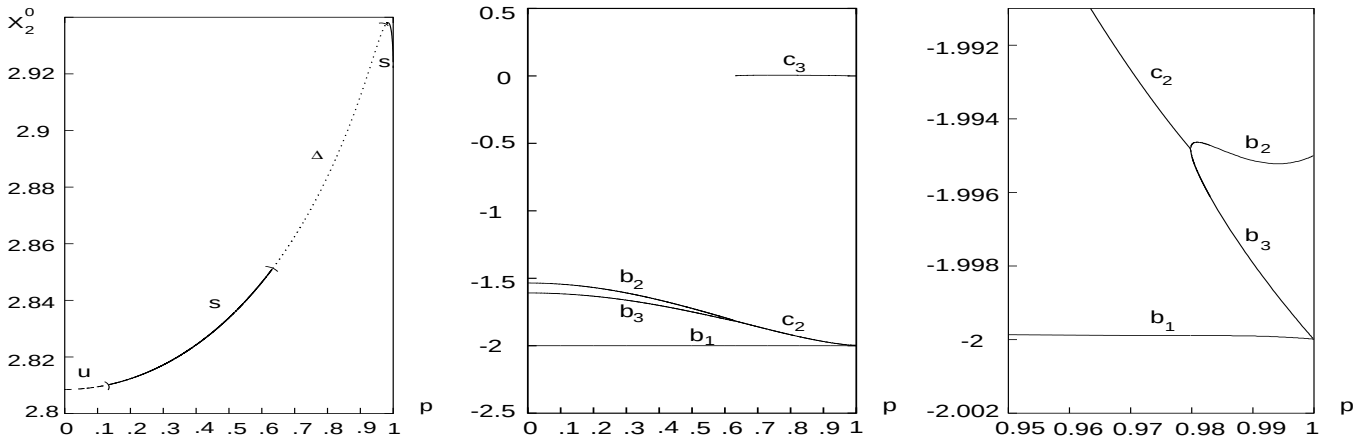

Fig. 12a. **Fig. 12b.** **Fig. 12c.**

Fig. 12. Family F^1_{50}. Actually parameter b_2 is always greater than -2. We remark the two transitions S-Δ in **b** and **c**.

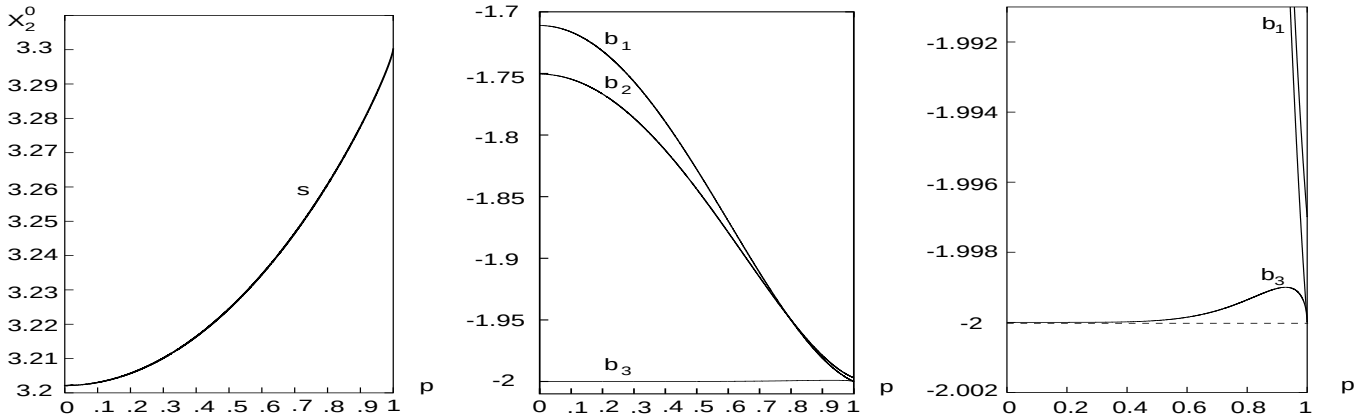

Fig. 13a. **Fig. 13b.** **Fig. 13c.**

Fig. 13. Family F^1_{60}. Figure **c** shows in detail the behavior of the third index, b_3, close to $p = 1$.

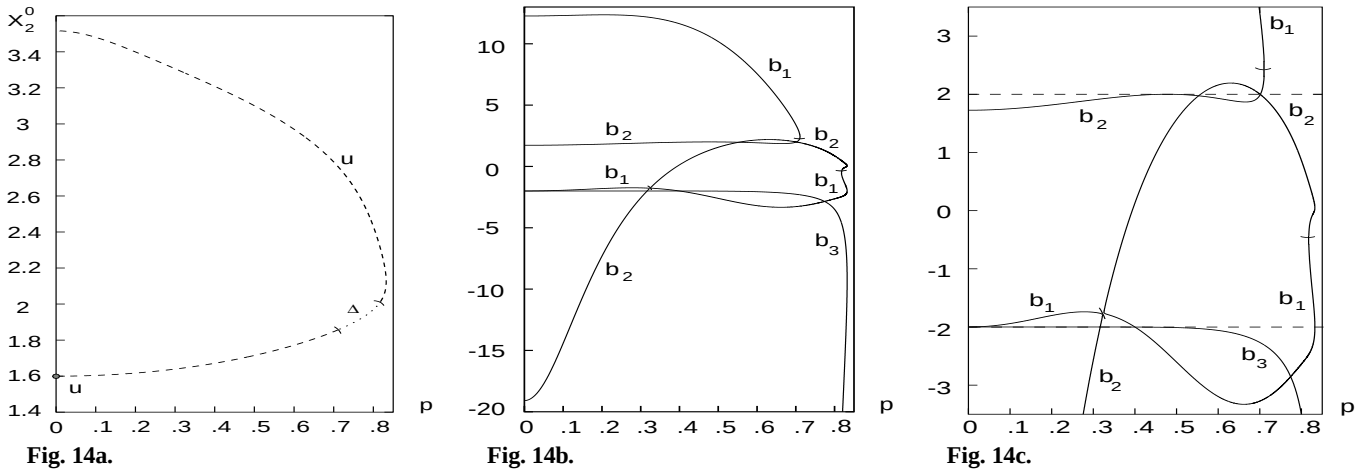

Fig. 14a. **Fig. 14b.** **Fig. 14c.**

Fig. 14. Families F^2_{50} and F^2_{51} are the same. In figure **a** the initial orbit of F^2_{50} is pointed with a bullet (•). In fact, there is a short complex unstable zone for $0,3221 \leq p \leq 0.3257$, which is not visible in figure **a**, but is marked with a segment (\) in figure **c**. The values c_i and c_j for the complex unstable orbits have been omitted for the sake of clarity. We mark the transitions to Δ by curvilinear segments ($\smile$).

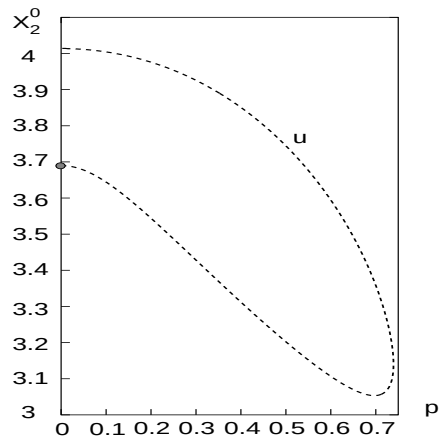

Fig. 15a.

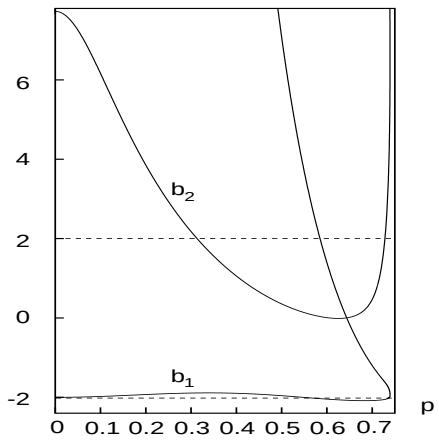

Fig. 15b.

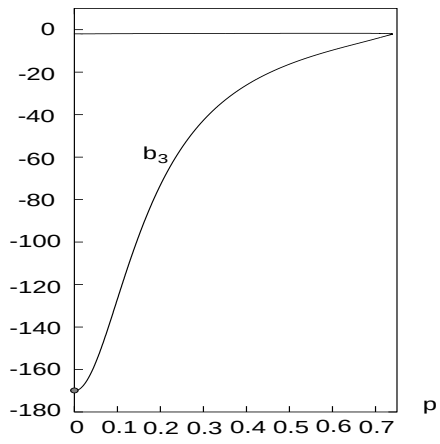

Fig. 15c.

Fig. 15. Family F^1_{31}. Indices b_1 and b_2 grow as the family turns back and p goes to zero, so the family becomes highly unstable, (in **b** only a range between -2.4 and 7.8 is plotted). In **a**, and **c**, the initial orbit is marked with a bullet (•).

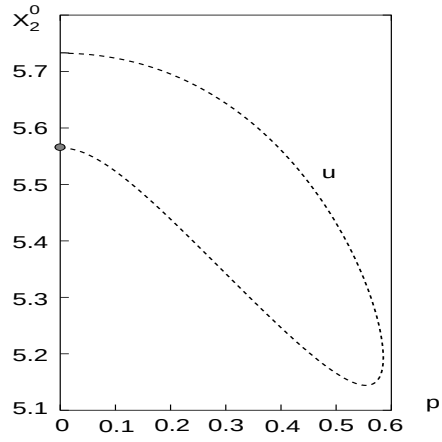

Fig. 16a.

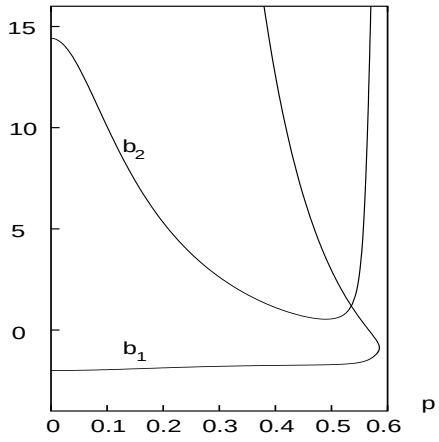

Fig. 16b.

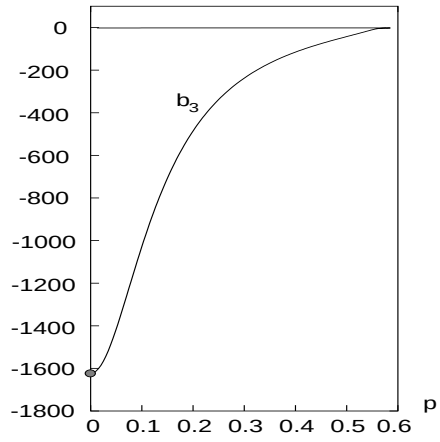

Fig. 16c.

Fig. 16. Family F^1_{51}. It is quite similar to the family F^1_{31}. In **a** and **c** the initial orbit is marked with a bullet.

4. The Sitnikov problem

As mentioned in the introduction, this is a special case of the Three Dimensional ERTBP. We assume now that the particle moves on the axis perpendicular to the orbital plane of the primaries, which move on Keplerian ellipses with eccentricity $e \in [0,1]$, around their center of gravitation.

From equations (6), we obtain that the equations of motion of the particle in coordinates z, $\dot z$ become

$$\frac{\mathrm{d}z}{\mathrm{d}E} = (1+e\cos E)\,\dot z,$$

$$\frac{\mathrm{d}\dot z}{\mathrm{d}E} = (1+e\cos E)\left\{\frac{-z}{\left[z^2+\frac{1}{4}\left(1+e\cos E\right)^2\right]^{\frac{3}{2}}}+\frac{C^2}{z^3}\right\}.$$

In section 2 periodic orbits of the Sitnikov Problem for $e = 1$ have been obtained as limiting orbits of the Planar Isosceles Restricted Problem (with $C = 0$). Therefore, each periodic orbit with initial conditions z_0, $\dot z_0 = 0$ and period $T = 2k\pi$, $k \in \mathbb{N}$, can be continued when varying the eccentricity e from 1 to 0, giving a periodic orbit of the Sitnikov Problem with the corresponding e. We denote these families by S_k and we show, for example, families S_4 and S_8 that start at orbits SB^1_2 and SB^1_4 in Fig. 20 and in Fig. 21.

On the other hand, we can also generate periodic orbits of the Sitnikov Problem just beginning at the Circular Sitnikov Problem (MacMillan Problem, which corresponds to $e = 0$). In this problem, there is a family of periodic orbits with increasing period $T > \pi/\sqrt{2}$ (see Belbruno et al. 1994). So, we have selected those ones of period $2k\pi$, $k \in \mathbb{N}$, and we have followed them for any e between 0 and 1, generating new families S_k. We show in Fig. 17, 18 and 19, the characteristic curves of families S_1, S_2 and S_3. Therefore, for fixed values of the period

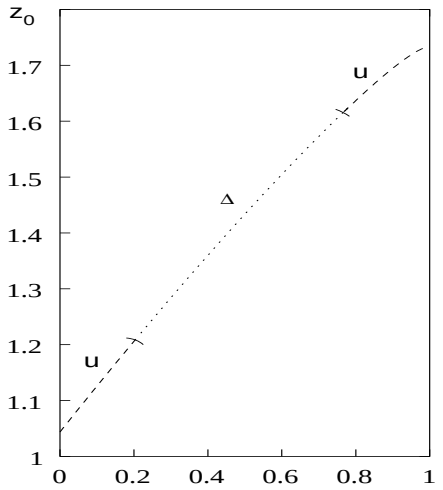

Fig. 17a.

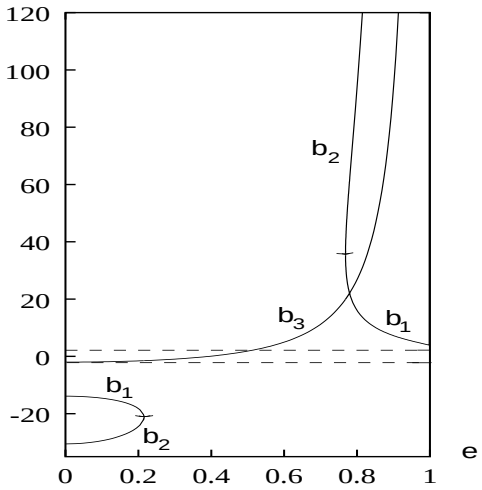

Fig. 17b.

Fig. 17. a characteristic curve of the Sitnikov family S_1. Here, the initial condition z_0 ($\dot{z}_0 = 0$), is plotted in front of e; the eccentricity of the primaries. In **b** we draw the stability indices. The complex unstable indices c_1 and c_2 have been omitted, and the points corresponding to transitions towards complex instability are marked with curvilinear segments.

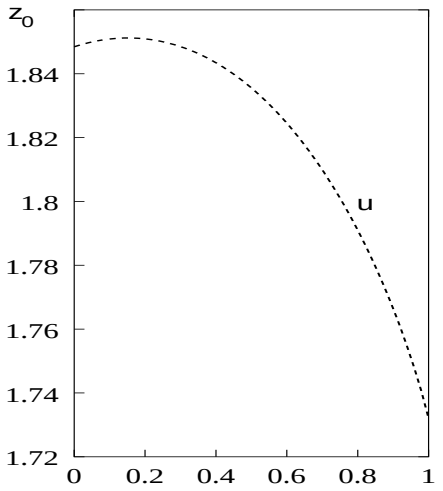

Fig. 18a.

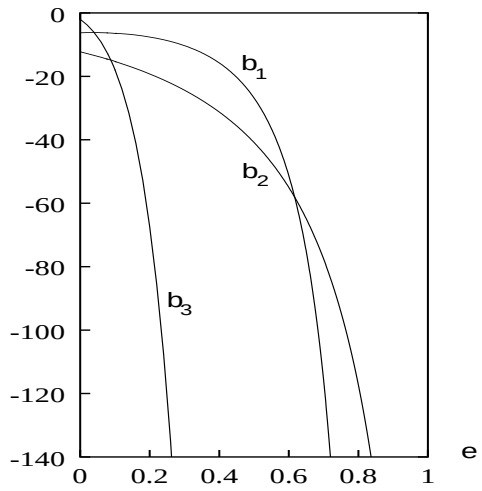

Fig. 18b.

Fig. 18. a characteristic curve of the Sitnikov family S_2. **b** stability indices.

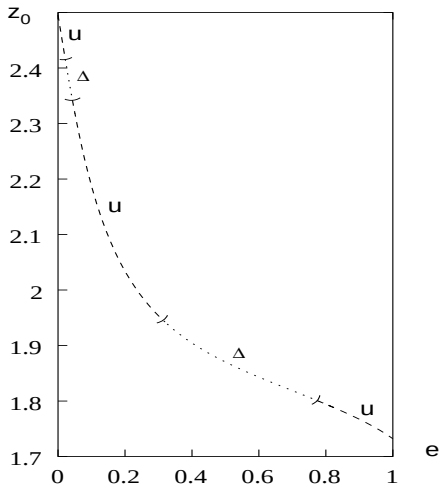

Fig. 19a.

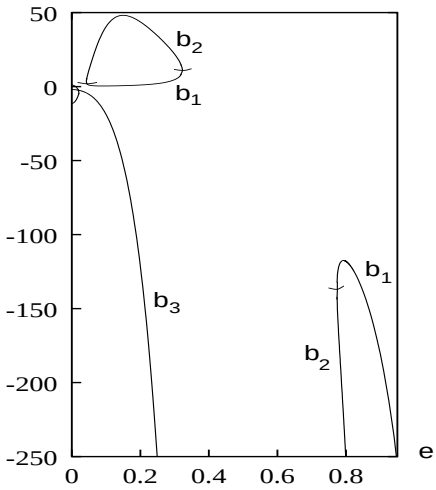

Fig. 19b.

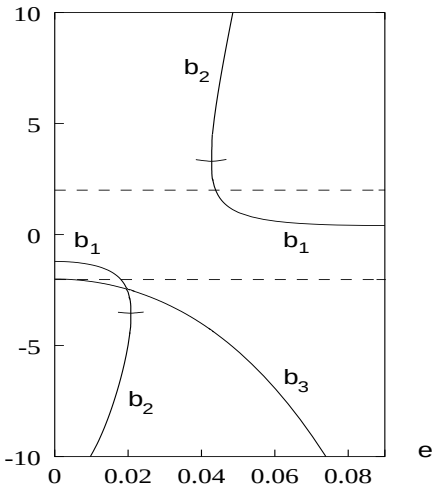

Fig. 19c.

Fig. 19. a characteristic curve of the Sitnikov family S_3. **b** stability indices. In **c** we show the stability indices for small values of e. In both figures the complex unstable indices c_1 and c_2, have been skipped, while transitions to Δ are marked with curvilinear segments.

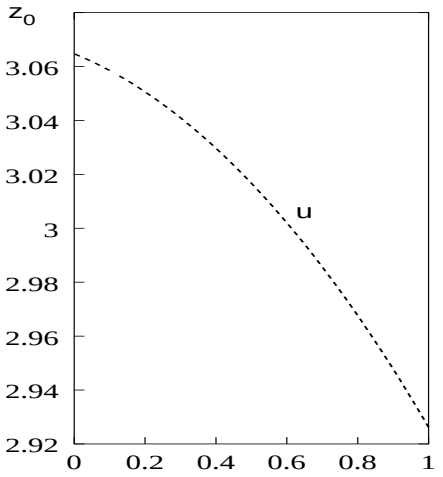

Fig. 20a.

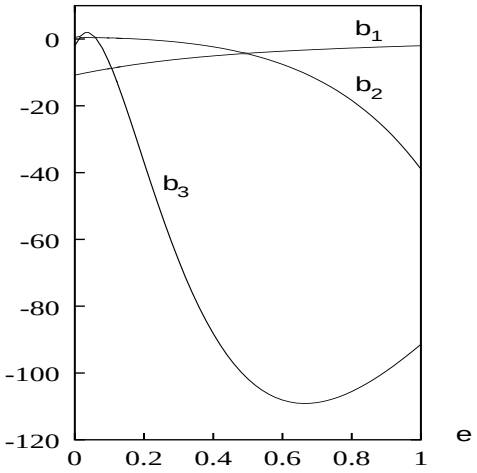

Fig. 20b.

Fig. 20. a characteristic curve of the Sitnikov family S_4. The initial condition z_0 is plotted against the eccentricity of the primaries e. In **b** we give the stability indices of the family.

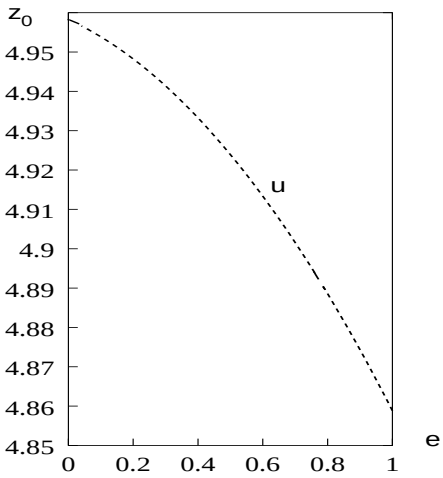

Fig. 21a.

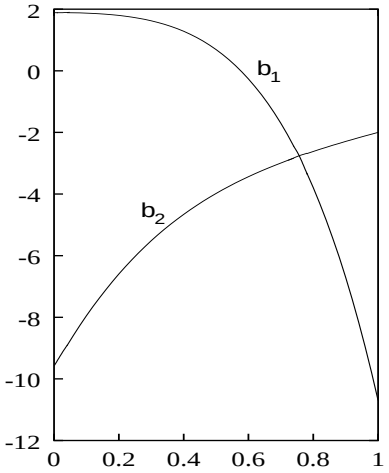

Fig. 21b.

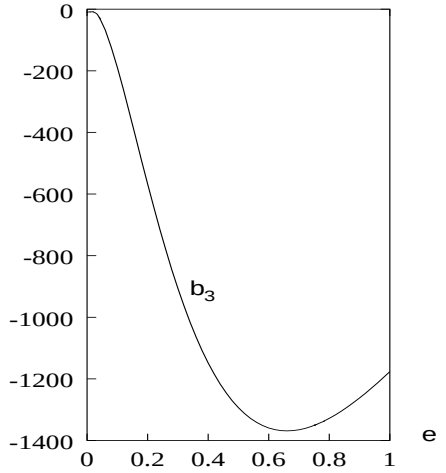

Fig. 21c.

Fig. 21. a characteristic curve of the Sitnikov family S_8. **b** shows the two first indices b_1, b_2, and in **c** the third index, b_3 is plotted with respect to e.

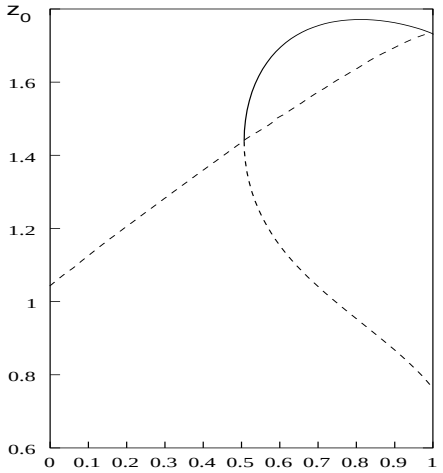

Fig. 22a.

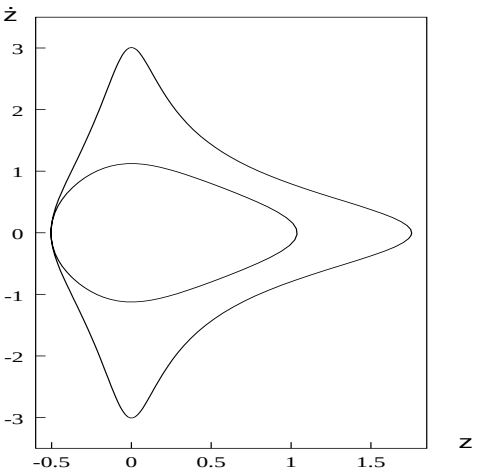

Fig. 22b.

Fig. 22. a bifurcated families from the S_1 (central branch in the diagram). One of them is drawn in thick continuous line, while the other, which corresponds to the *same* family – see the text –, has been plotted with thick dashed lines. **b** example of an orbit on the bifurcated family.

Table 4. Stability parameters of families S_1, S_2, S_3, S_4, and S_8.

Family	z_0 for $e=0$	z_0 for $e=1$	# of critical orbits
S_1	1.0436980426	$\sqrt{3}$	1
S_2	1.8484596137	$\sqrt{3}$	0
S_3	2.4953935525	$\sqrt{3}$	3
S_4	3.0647130981	2.9261824967	2
S_8	4.9582234542	4.8588359848	3

$T = 2k\pi$ and the eccentricity e, each periodic orbit computed is a particular orbit of the ERTBP.

We plot from Fig. 17 to 21 the stability parameters computed for the families S_k, $k = 1, 2, 3, 4, 8$. When e is close to 1, the periodic orbits become very unstable. Actually, families S_1, S_2 and S_3 end at a triple collision orbit, the so called *equilateral one* (see Álvarez, 1997). Also, we remark several transitions to complex instability for families S_1 and S_3. Finally we give in table 4 the initial condition z_0 of the limiting orbits for $e = 0$ and $e = 1$, as well as the number of critical orbits of each family.

As mentioned above, any critical orbit is a candidate to bifurcate to other families of periodic orbits. For example, family S_1 has one critical orbit of period 2π, which does bifurcate to two other families S_1^a and S_1^b of periodic orbits of period 4π again in the Sitnikov Problem. Actually both families become the same – we call them $\mathrm{S}_1^{4\pi}$ –, since for any value of e, the corresponding orbit $(z(E), \dot{z}(E))$ of S_1^a with the initial value z^a (and $\dot{z}_0 = 0$) satisfies $z(2\pi) = z_0^b$, $\dot{z}(2\pi) = 0$. That is, the initial condition of the corresponding orbit belonging to S_1^b. This family ends, for $e = 1$, at two different triple collision orbits: the equilateral one (limiting orbit of the upper branch) and the other one for which the triple collision takes place when $E = \pi$ (limiting orbit of the lower branch). In Fig. 22a we plot the characteristic curve of the bifurcated family; and a sample orbit of the bifurcated family in Fig. 22b.

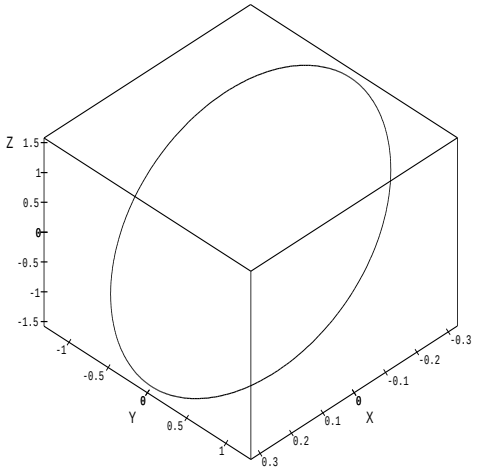

Fig. A1a. F_{20}^1

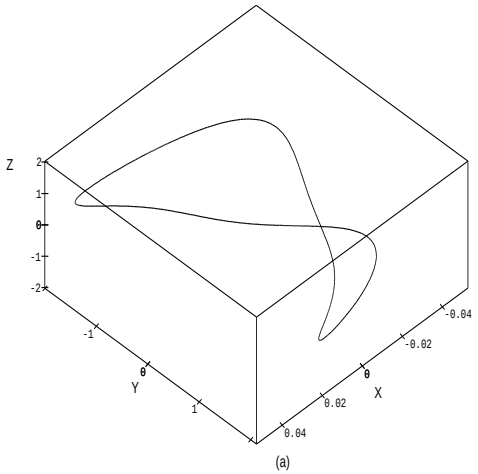

Fig. A1b. F_{30}^1

5. Conclusions

We have shown a channel to connect different limiting Restricted Problems in order to generate families of periodic orbits in the Spatial Elliptic RTBP. On one hand, we have computed some families of solutions of the Planar Isosceles Restricted Problem, which contain *real* periodic orbits. These orbits have been continued in the parameter e, and we have obtained families of periodic orbits of the Spatial Elliptic RTBP. On the other hand, the Sitnikov Problem has been considered to link the MacMillan problem with the PIRP. For the SP when e varies from 0 to 1, some families of periodic orbits (as particular solutions of the ERTBP) were computed.

For the ERTBP, an stability analysis of the periodic orbits computed, shows that they are mostly unstable and transitions to complex instability appear quite naturally. More concretely, only three transitions from stability to complex instability were found. One in the family F_{30}^1, while the other two belong to F_{50}^1 (see Fig. 10c and Fig. 12b, c). The bifurcations associated with the three transitions turn out to be *direct* Hopf-like bifurcations. This implies the existence of stable 2D tori as well as "long-time" confinement (given by the stable and unstable invariant manifolds of the complex unstable orbit) close to the unstable orbit. Actually, in the Circular 3D RTBP we had shown the existence of confinement and computed the bifurcated 2D tori in a neighborhood of complex unstable periodic orbits near the Lagrangian points for $\mu > \mu_{Routh}$ (see Ollé and Pacha, 1998). The present paper is the starting point for studying a rich dynamical behavior expected close to the transitions to complex instability in the ERTBP.

Appendix A: Gallery of periodic orbits

We show (Fig. A1a to A1d), some typical orbits belonging to the families of the ERTBP obtained in section 3. All of them correspond to a value of $p = 0.5$, and the family which contains the orbit is specified at the bottom of the figure.

Acknowledgements. This work has been supported by the Catalan grant CIRIT 1998S0GR-00042.

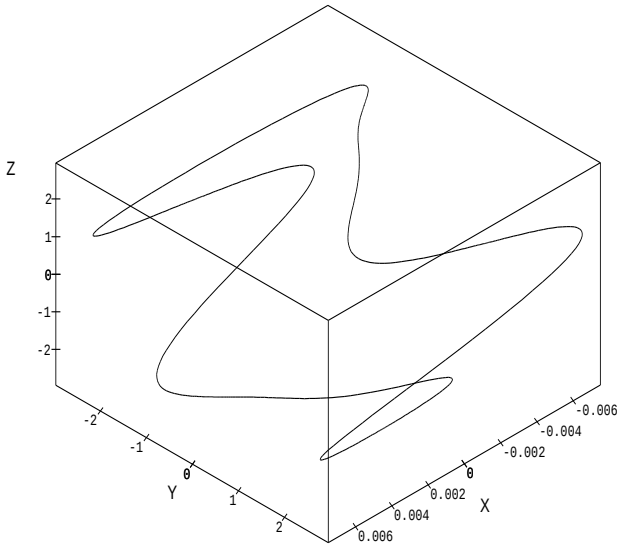

Fig. A1c. F_{50}^{1}

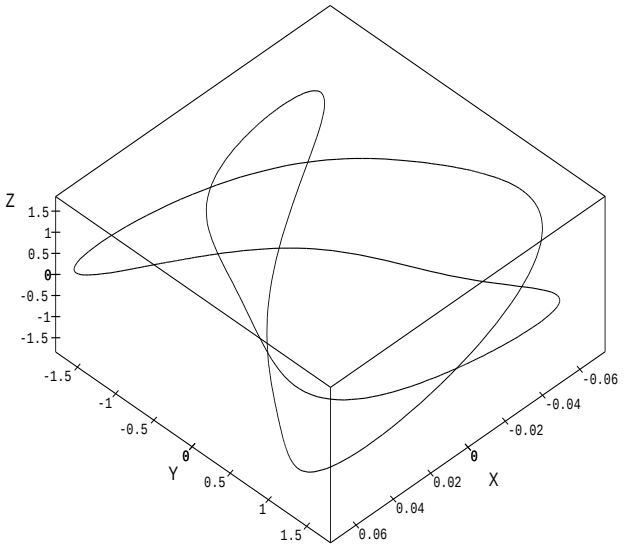

Fig. A1d. F_{50}^{2}

References

Álvarez, M., 1997, PhD Thesis, Univ. Autònoma de Barcelona

Belbruno, E., Llibre, J., Ollé, M., 1994, Cel. Mech. 60, 99

Broucke, R. A., 1969, AIAA journal 6, 1003

Broucke, R. A., 1971, Mécanique 10, 449

Broucke, R. A., 1979, A&A 73, 303

Bridges, T. J., Cushman, R. H., Mackay, R. S., 1995, Fields Inst. Comm. 4, 61-73

Cleary, P. W., 1989, ApJ 337, 108

Contopoulos, G., 1986a, A&A 161, 244

Contopoulos, G., 1986b, Cel. Mech. 38, 1

Contopoulos, G., 1988a, Cel. Mech. 44, 393

Contopoulos, G., 1988b, Cel. Mech.

Contopoulos, G., Barbanis, B., 1985, A&A 153, 44

Contopoulos, G., Barbanis, B., 1994, Cel. Mech. and Dynam. Astron. 59, 279

Contopoulos, G., Giorgilli, A., 1988, Meccanica 23, 19

Contopoulos, G., Farantos, S. C., Papadaki, H., Polymilis, C., 1994, Phys. Rev. E 50, 6, 4399

Dvorak, R., 1993, Cel. Mech. and Dynam. Astron. 56, 71

Gómez, G., Llibre, J., Martínez, R., Simó, C., 1985, Station Keeping of Libration Point Orbits, ESOC Report 5648/83/D/JS(SC)

Gómez, G., Jorba, A., Masdemont, J., Simó, C., 1992, Study of Poincaré maps for Orbits near Lagrangian Points, ESOC Report 9711/91/D/IM(SC)

Hagel, J., 1992, Cel. Mech. and Dynam. Astron. 53, 267

Hagel, J., Trenkler, T., 1993, Cel. Mech. and Dynam. Astron. 56, 81

Hadjidemetriou, J. D., 1985. In: Resonances in the Motion of Planets, Satellites and Asteroids. Ferraz-Mello, S. (ed.) Univ. of Sao Paulo

Heggie, D.G., 1985, Cel. Mech. 35, 357

Jorba, A., Villanueva, J., 1997, Nonlinearity, 10, 783-882

Katsiaris, G., 1973, The Three Dimensional Elliptic Problem. In: Recent Advances in Dynamical Astronomy, p. 118–134

Liu, J., Yi-Sui Sun, 1990, Cel. Mech. 49, 285

Llibre, J., Simó, C., 1980, Actas II C.E.D.Y.A., Publ. Mat. UAB, 49

Macris G., Katsiaris, G. A., Goudas, C. L., 1975, Ap&SS 33, 333-340

MacMillan, W. D., 1913, AJ 27, 11

Magnenat, P., 1982a, Cel. Mech. 28, 319

Magnenat, P., 1982b, A&A 108, 89

Martinet, L., Pfenniger, D., 1987, A&A 173, 81

Martinet, L., de Zeeuw, T., 1988, A&A 206, 269

Martínez Alfaro, J., Chiralt, C., 1997, Cel. Mech. and Dynam. Astron. 55, 351

Martínez Alfaro, J., Orellana, R.B., 1997, Cel. Mech. and Dynam. Astron. 67, 275

Moser, J., 1973, Stable and Random Motions in Dynamical Systems. Annals of Math. Studies 77, Princeton University Press.

Ollé, M., Pacha, J. R., 1998, Motion Near the Transition to Complex Instability: Some Examples. In: Actas del XV Congreso de Ecuaciones Diferenciales y Aplicaciones, Vol. I. Univ. de Vigo (ed.)

Ollé, M., Pfenniger, L., 1998, A&A 334, 829-839

Ollé, Pacha, J. R., Villanueva, J., 1999, in preparation

Pacha, J. R., 1999, PhD Thesis, in progress

Papadaki, H., Contopoulos, G., Polimilis, C., 1995, Complex instability. In: From Newton to Chaos, Roy, A.E., Steves, B.E. (eds.), Plenum Press, New York, 485

Patsis, P. A., Zachilas, L., 1990, A&A 227, 37

Patsis, P. A., Zachilas, L., 1994, Intern. J. Bif. and Chaos 4, No. 6, 1399

Pfenniger, D., 1985a, A&A 150, 97

Pfenniger, D., 1985b, A&A 150, 112

Pfenniger, D., 1987, A&A 180, 79

Pfenniger, D., 1990, A&A 230, 55

Poincaré, H.: 1899, Les Méthodes Nouvelles de la Mécanique Céleste, Gauthier-Villars, Paris

Puel, F., 1979, Cel. Mech. 20, 105

Sitnikov, K., 1960, Dokl. Akad. Nauk. USSR 133, 303

Waldvogel, J., Cel. Mech. 8, 189

Wodnar, K., 1992, The original Sitnikov article. New insights, Master-Thesis, Univ. of Viena.

Zachilas, L., 1993, A&AS 97, 549